ELSEVIER

Journal of Structural Geology 29 (2007) 1665–1678

JOURNAL OF STRUCTURAL GEOLOGY

www.elsevier.com/locate/jsg

Modeling the influence of tectonic extrusion and volume loss on the geometry, displacement, vorticity, and strain compatibility of ductile shear zones

Graham B. Baird*, Peter J. Hudleston

Department of Geology and Geophysics, University of Minnesota, Minneapolis, MN 55455, USA

Received 15 November 2006; received in revised form 31 May 2007; accepted 22 June 2007
Available online 6 August 2007

Abstract

Oblate strains are often observed in meso-scale ductile shear zones and this is generally taken to indicate narrowing across the shear zone during formation. Volume loss is one mechanism that could produce shear zone narrowing. However, not all shear zones display characteristics consistent with volume loss, and in such cases, the narrowing must be accomplished by the extrusion of material from within the shear zone. To explore the relationship between shear zone geometry, volume loss, and extrusion, shear zones were mathematically modeled. Results demonstrate the important influence of pure shear and volume loss on controlling the geometry, displacement, and vorticity of ductile shear zones. Further, volume loss does not preclude extrusion unless, for a given volume loss, the strain is of a specific geometry. Extrusion is a likely mechanism important in shear zone development, even if volume loss occurs. Extrusion presents strain compatibility problems because, unlike crustal-scale shear zones, meso-scale ductile shear zones do not possess a free surface. If extrusion occurs, bulk strain compatibility can be maintained if shear zones interlink in anastomosing arrays or change in thickness, though not all shear zone systems display such characteristics. Modeling results elucidate the deformation style of shear zone in the northwest Adirondacks in NY and in the Kebnekaise region in northern Sweden.

Keywords: 3D strain; Volume loss; Ductile shear zones; Strain compatibility; Modeling

1. Introduction

Ductile shear zones are tabular zones of high strain bounded by relatively un-deformed wall rock and are typical manifestations of rock deformation (Fig. 1). Early work with shear zones suggested that heterogeneous simple shear is their typical characteristic deformation style (e.g. Ramsay and Graham, 1970; Cobbold, 1977; Ramsay and Allison, 1979; Ramsay, 1980; Simpson, 1983). Typically when shear zones are studied they are considered to have parallel sides, lack discontinuities, and the walls of the shear zone remain undeformed prior to, during, and after shear zone development. If this is accurate, then in reality the shear zone can be formed by any heterogeneous combination of pure shear and simple shear, with or without volume change (e.g. Ramsay and Graham, 1970; Ramsay, 1980; Ramsay and Huber, 1987). In the case of pure shear, this can be a disfavored scenario as it potentially violates strain compatibility (e.g. Ramsay and Graham, 1970; Ramsay, 1980; Hudleston, 1999).

In the classic Ramsay and Graham (1970) model of shear zone formation, simple shear is the only mechanism responsible for its formation and this should yield plane strain (e.g. Hudleston, 1999). However, a survey of detailed analyses of shear zones indicates many cases where the deformation deviates from simple shear (e.g. Coward, 1976; Grunsky et al., 1980; Choukroune and Gapais, 1983; Mohanty and Ramsay, 1994; Srivastava et al., 1995; Ring, 1999; Bhattacharyya and

* Corresponding author: Earth Sciences, University of Northern Colorado, Greeley, CO 80639, USA. Tel.: +1 970 351 2830; fax: +1 970 351 4197.
E-mail address: graham.baird@unco.edu (G.B. Baird).

0191-8141/$ - see front matter © 2007 Elsevier Ltd. All rights reserved.
doi:10.1016/j.jsg.2007.06.012

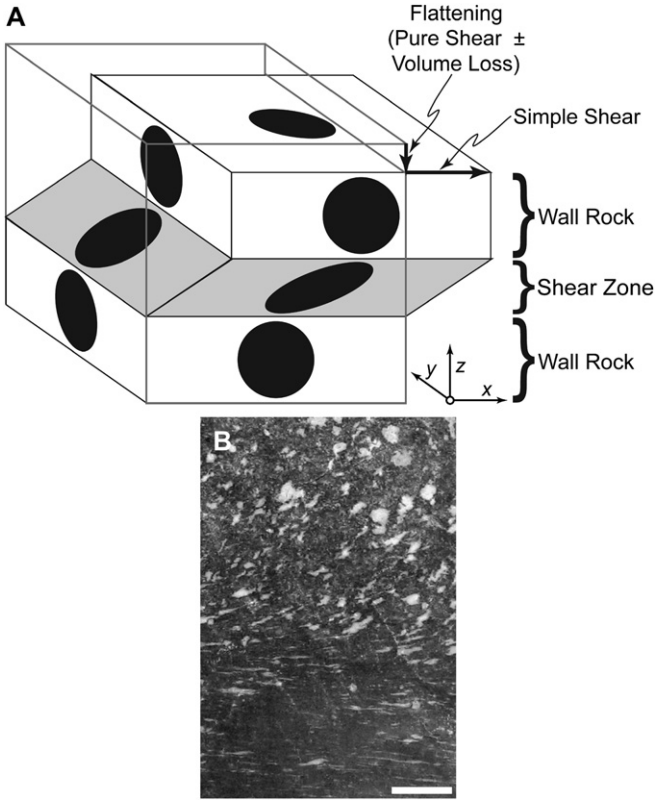

Fig. 1. (A) Idealized model of a ductile shear zone with strain markers. In this analysis, the wall rock bounding the shear zone remains undeformed prior to, during, and following shear zone development. Shear zone geometry not representative of a pure shear deformation component, see text for details. (B) Strain gradient in a natural ductile shear zone from the Tarfala Valley, northern Sweden. Scale bar is 2 cm.

Hudleston, 2001). Oblate strains are common and dissolution volume loss, the removal of material from within the shear zone by syn-shearing fluids, is often cited as the mechanism that produces the oblate strains (e.g. Grunsky et al., 1980; O'Hara, 1990; Ring, 1999; Mohanty and Ramsay, 1994). This should lead to a narrowing or flattening of the shear zone during deformation (Fig. 1A). Often the evidence for volume loss is equivocal (c.f. Simpson, 1981; Mohanty and Ramsay, 1994), and in some cases, volume loss can be discounted (Srivastava et al., 1995; Bhattacharyya and Hudleston, 2001).

If conditions for deformation are isochoric (constant volume), then lateral displacement of shear zone material must occur to create oblate strain and the shear zone will narrow. This, however, creates strain compatibility problems (see Hudleston, 1999; Bhattacharyya and Hudleston, 2001). The lateral movement of material may be called tectonic extrusion or tectonic intrusion, depending upon the direction of material movement relative to the shear zone. The evidence for extrusion and intrusion can be controversial and, so far, structures associated with extrusion and intrusion has not unequivocally been identified. Complete 3D strain analysis, including both strain ellipsoid shape and ellipsoid orientation relative to the shear zone boundary, augmented by volume loss estimations, are required to fully assess the style of deformation and the degree of extrusion and intrusion associated with a shear zone.

This contribution explores models of narrowing shear zones during deformation referred to as "transpression" (e.g. Sanderson and Marchini, 1984). Thickening shear zones, due to some combination of volume change and intrusion are possible, evidence for these are not wide spread and will not be focused upon. The specific role of volume loss in influencing extrusion and intrusion is of special interest. Results demonstrate that only in unique situations can extrusion and intrusion be ruled out to explain a specific strain. Evidence for extrusion can be obtained independently of strain analyses and some examples will be shown. Also, some shear zone systems are isochoric and show no evidence for extrusion. In such cases, deformation must be by simple shear.

2. Methods

Many attempts at integrating strain analyses with volume loss estimates have been plagued by incomplete strain analysis and/or inaccurate volume loss estimates. These problems can be a result of an incomplete understanding of strain development due to an inability to properly model the characteristics of progressive deformation via simultaneous simple shear and pure shear, with or without volume loss. Recent techniques (Fossen and Tikoff, 1993; Tikoff and Fossen, 1993) allow these types of progressive deformations to be explored. Application of these techniques (e.g. Fossen et al., 1994; Tikoff and Greene, 1997; Teyssier and Tikoff, 1999; Tikoff and Fossen, 1999) and other techniques (e.g. Sanderson and Marchini, 1984; Robin and Cruden, 1994; Dutton, 1997; Jones et al., 1997) have been used fairly extensively to model the strain and fabrics of crustal-scale shear zones that possess a free surface. Such models can accommodate extrusion and intrusion easily. Volume loss and strain compatibility are much less of an issue with crustal-scale shear zones. The models presented here, strictly speaking, are scale independent, although scale is involved in some circumstances to emphasize the consequences of scale on displacement of material in meso-scale ductile shear zones.

2.1. Mathematical approach

Fossen and Tikoff (1993) and Tikoff and Fossen (1993), following the original work of Ramberg (1975), present the mathematics and derivation of key equations applied to the modeling of tabular shear zones. The monoclinic shear zone reference frame constructed for this analysis places the x- and y-axes in the plane of the shear zone with z normal to the shear zone (Fig. 1A). Simple shear is constrained to be in the x-direction. With these constraints, a deformation leading to some total strain, D, is described by the deformation matrix:

$$D = \begin{bmatrix} k_x & 0 & \Gamma \\ 0 & k_y & 0 \\ 0 & 0 & k_z \end{bmatrix}, \tag{1}$$

where k_x, k_y, and k_z are the reference frame coaxial stretch in the x, y, and z-directions respectively. Γ is the effective shear strain, which is a function of k_x, k_z, and γ, the simple shear

component in the x-direction. For this reference frame with simultaneous simple shear and pure shear deformation, Tikoff and Fossen (1993) demonstrated that the effective shear strain is:

$$\Gamma = \gamma \frac{(k_x - k_z)}{\ln(k_x/k_z)}. \tag{2}$$

The eigenvalues (λ_1, λ_2, and λ_3, where $\lambda_1 \geq \lambda_2 \geq \lambda_3$) of a deformation matrix determine the lengths of the three quadratic principal strain ellipsoid axes, where $\lambda = (1+e)^2$. They are determined by (Fossen and Tikoff, 1993):

$$\lambda_{1,\ 2,\ \text{or}\ 3} = \frac{\Gamma^2 + k_x^2 + k_z^2 + \sqrt{-4k_x^2k_z^2 + \left(\Gamma^2 + k_x^2 + k_z^2\right)^2}}{2}, \tag{3A}$$

$$\lambda_{1,\ 2,\ \text{or}\ 3} = \frac{\Gamma^2 + k_x^2 + k_z^2 - \sqrt{-4k_x^2k_z^2 + \left(\Gamma^2 + k_x^2 + k_z^2\right)^2}}{2}, \tag{3B}$$

and

$$\lambda_{1,\ 2,\ \text{or}\ 3} = k_y^2. \tag{3C}$$

The equation that yields a specific quadratic principal ellipsoid axis (λ_1, λ_2, and λ_3) is not known *a priori* without knowing the values of k_x, k_y, k_z, and γ.

The kinematic vorticity (W_k) is a useful number that describes the relative contribution of simple shear and pure shear to a deformation. It is defined as (Fossen and Tikoff, 1993):

$$W_k = \gamma\left\{2(\ln k_x)^2 + 2(\ln k_z)^2 + \gamma^2\right\}^{-0.5}, \tag{4}$$

and its value is between 1 (all simple shear) and 0 (all pure shear) for a deformation matrix and is the same for all increments of a particular deformation. As will be shown, volume change does have some effect on W_k.

The R-θ' diagram is a method, given the finite strain of a shear zone, to determine the contribution of simple shear plus other deformation styles to the finite strain (Fig. 2). The diagram displays the strain ellipse geometry in the plane perpendicular to the shear zone walls and parallel to the shear direction – here the xz-plane. The resulting strain from a deformation matrix can be plotted on this diagram using the following definitions: R is the aspect ratio of the strain ellipse:

$$R = \sqrt{\lambda_{xz\text{Max}}/\lambda_{xz\text{Min}}}, \tag{5}$$

where $\lambda_{xz\text{Max}}$ and $\lambda_{xz\text{Min}}$ are the greatest and least eigenvalues or squared strain ellipse axis length in the xz-plane respectively (Eqs. (3A) and (3B)); and θ' is the angle between the long axis of the strain ellipse and the shear plane (Tikoff and Fossen, 1993):

$$\theta' = \arctan\left(\frac{\Gamma^2 + k_x^2 - \lambda_{xz\text{Max}}}{-k_z\Gamma}\right). \tag{6}$$

It is important to note that R-θ' states of strain are only a 2D representation of the strain ellipsoid from a shear zone or a deformation matrix. Contoured across the diagram are values of shear strain (γ) and Δ_{ap}. Δ_{ap} has been labeled Δ by other workers (Fossen and Tikoff, 1993) because in the specific situation of $k_x = k_y = 1$, Δ_{ap} is equal to the volume change (Δ) of the deformation – as well as the area change of the strain ellipse in the xz-plane. Here, this parameter is labeled Δ_{ap} to more generally indicate the *apparent* area change of the strain ellipse in the xz-plane based on the ellipse's shape and orientation. This apparent area change could be due to any combination of pure shear and volume change.

This paper focuses on the geometric significance of volume change to shear zone geometry, so it is important to clarify that Δ_{ap}, strictly speaking, defines the relationship of k_x to k_z. Δ_{ap} is positive when k_z is greater than k_x and Δ_{ap} is negative when k_z is less than k_x. That is:

$$k_z = k_x\left(1 + \Delta_{ap}\right), \tag{7}$$

while the true volume change (Δ) for any particular deformation is determined by:

$$\Delta = \sqrt{k_x^2 + k_y^2 + k_z^2} - 1. \tag{8}$$

Note that when $\Delta_{ap} = 0$, then the deformation is by simple shear only, if it is isochoric ($\Delta = 0$; dotted line of Fig. 2). The specific details of how a volume change affects the strain ellipsoid shape is not directly investigated in this work and it can generally be thought of dilation.

2.2. R-θ' diagram and the Flinn diagram

Stretch in the y-axis (k_y) is independent of k_x and k_z (Bhattacharyya and Hudleston, 2001) such that the R-θ' diagram state of strain provides no insight to the magnitude of k_y. Therefore, for any 2D R-θ' state of strain, there is a set of possible corresponding Flinn diagram states of strain. Fig. 3 summarizes all possible Flinn diagram states of strain that correspond to an R of 4.0 and a θ' of 26.6°, which is the state of strain produced by simple shear with $\gamma = 1.5$. This diagram was created by varying k_y from very large values to very small values and it demonstrates the necessity of a full 3D strain analysis, including θ' measurement, in order to uniquely define the style of deformation – first alluded to by Bhattacharyya and Hudleston (2001). Typically strain analyses do not measure absolute strain such that the dilation (volume change) of a particular deformation is not known. That is, given a state of strain, there is an infinite number of ellipsoids of varying size, representing various volume changes, that are indistinguishable when plotted on the R-θ' diagram and Flinn diagram. Typical strain analyses are thought to provide relative strain where the shape and orientation of the finite strain is accurately known but the volume change is not.

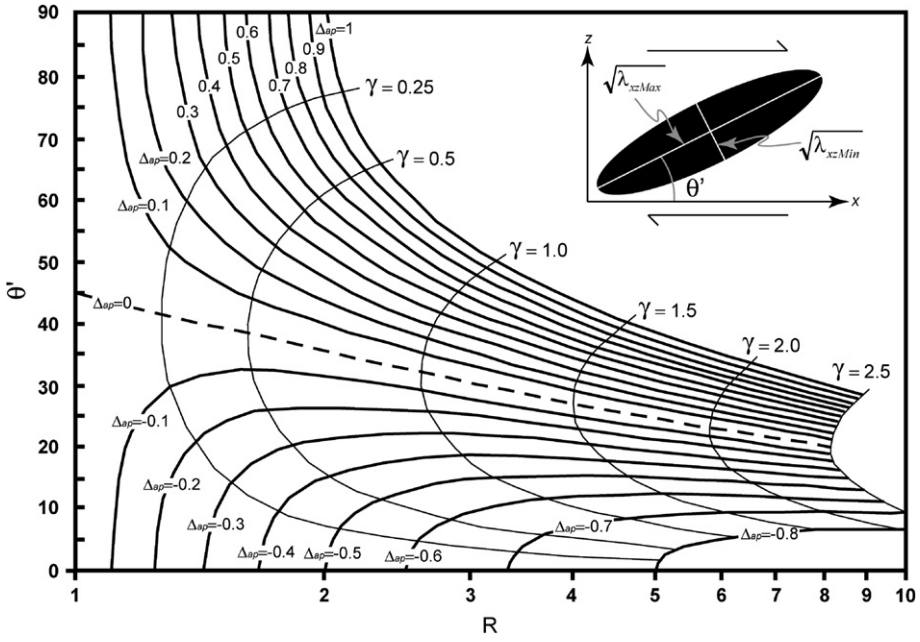

Fig. 2. The ever-popular R-θ' diagram of simultaneous simple shear, pure shear and/or volume change (after Fossen and Tikoff, 1993). Δ_{ap} is used here where these contours are labeled as Δ in Fossen and Tikoff (1993). This emphasizes that volume change is only one mechanism by which strain can deviate from the simple shear line ($\Delta_{ap} = 0$). Inset defines variables used in the plot, R defined by Eq. (5), see text for details.

2.3. Deformation matrix from strain data

Given a finite strain determined by any number of means, such as the R_f/Φ method (Lisle, 1985), the matrix that describes the deformation resulting in the strain is easily obtained assuming a monoclinic deformation style and the constraints outlined above. The finite strain plotted on the R-θ' diagram provides the relationship of k_x to k_z, via Δ_{ap} (Eq. (7)), as well as γ. This quickly demonstrates the relative nature of most strain analyses as specific values of k_x, k_y, and k_z cannot be directly calculated and an iterative process must be employed to determine the required k_y for a given k_x, k_z, and γ to match the measured Flinn diagram strain. Volume change (Eq. (8)) of any deformation resulting from this iterative process may not be of the volume change of the measured/desired deformation. This is required to fully and accurately characterize the deformation. Any deformation matrix can be dilated (relative strain remains the same) to the desired volume change by the equation:

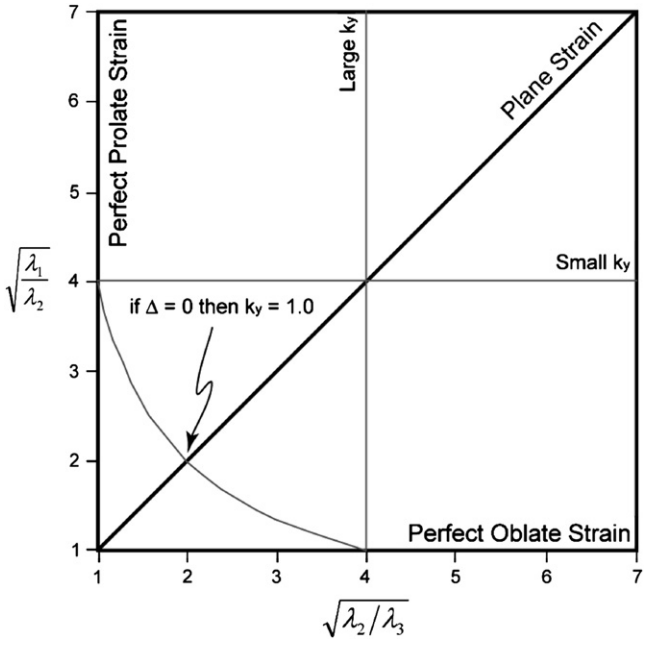

Fig. 3. Flinn diagram for all possible states of strain (gray line) corresponding to the R-θ' diagram state of strain where $\gamma = 1.5$ and $\Delta_{ap} = 0$.

$$F_d = \sqrt[3]{\frac{(1+\Delta_d)}{(1+\Delta_c)}}, \tag{9}$$

where F_d is the dilation factor, Δ_c is the current volume change of the deformation matrix (Eq. (8)), and Δ_d is the desired volume change for the deformation matrix. Multiplying F_d to each k_x, k_y, and k_z (γ remains the same) yields a deformation matrix that matches the measured strain on the R-θ' diagram, the Flinn diagram, and measured/desired volume change of the deformation. Measuring volume changes of deformations can be determined by the analysis of strain marker size, but more commonly, geochemical techniques are employed to estimate volume change.

2.4. Volume change determination through bulk chemistry

The isocon method (Grant, 1986) uses chemistry to estimate the volume change (e.g. O'Hara, 1990; Srivastava et al., 1995; Ring, 1999; Bhattacharyya and Hudleston, 2001; Yonkee et al., 2003). Volume losses are typically reported for shear

zones, though volume gain is possible. Critical in this method is to define the geochemical reference frame (Ring, 1999), meaning, identify the component(s) that have remained immobile during deformation, and in general, this assumes that components will behave differently during the volume change. Removal of mobile components during deformation will enrich the shear zone rock with the immobile components. Thus, the difference in concentration of the immobile component in the wall rock and shear zone is related to volume change by the equation (see O'Hara, 1990):

$$\Delta = \left(\frac{C_i}{C_f}\right) - 1, \tag{10}$$

where Δ is the volume change as described above, C_f is the "final" concentration (shear zone material); and C_i is the "initial" concentration (wall rock or protolith); so C_f/C_i is the slope of the immobile element(s) isocon (given that C_i is the x-axis and C_f is the y-axis). This version ignores density changes, which in most cases have been shown to be relatively small (Etheridge et al., 1983; O'Hara, 1990; Yonkee et al., 2003).

Fig. 4 displays a simple example where two components, A and B, make up the rock. Initially, they are in equal proportions, A is immobile while a quarter of B is lost during deformation. This enriches the shear zone in A while B is depleted in the shear zone and therefore the components plot above and below the isochemical line, respectively.

The isocon method certainly only provides an estimation of the volume loss and should not be considered as an exact measure, unless the perfectly immobile reference frame can be identified. The basic assumption that one or a few components remain immobile can be invalid in a number of different ways, each of which bears its own repercussions: (1) no components are immobile (all components are being lost or gained at some rate); in which case, the isocon method will underestimate the volume lost or gained. (2) Some components could be added to the shear zone and be misidentified as the immobile component; in this case the volume loss would be less than that indicated by the isocon method. (3) The chemical variations may not be related to shear zone development but could be a variation that existed prior to, or developed subsequent to, shear zone formation. In this case, any estimations of volume change based on the isocon method would be erroneous as the wall rock does not provide the proper reference frame. Unfortunately there is no way to determine if the chosen reference frame for the isocon method is truly correct, and different reference frame decisions can lead to vast differences in estimated volume loss (c.f. Simpson, 1981; Mohanty and Ramsay, 1994).

If major components do not vary between the shear zone and wall rock then the only way for there to be volume loss is if all the major elements were to be lost at a rate dictated by their initial concentration, which is geochemically unlikely (see data of e.g. Simpson, 1981; Bhattacharyya and Hudleston, 2001; Baird, 2006). If no major components lie on the line of constant concentration then is it likely that volume change has occurred (see data of Etheridge et al., 1983; O'Hara, 1990; Yonkee et al., 2003). Typically elements considered immobile are Ti, Al, and Zr, among others (e.g. Etheridge et al., 1983; O'Hara, 1990; Srivastava et al., 1995; Bhattacharyya and Hudleston, 2001; Yonkee et al., 2003).

2.5. Model construction

The model, based on collected absolute strain data from a natural shear zone (see above), provides information regarding displacement, change in shear zone thickness, and presence of intrusion/extraction, etc. For illustrative purposes, the shear zone model was constructed of three box-like slices, which will, following a prescribed deformation, become the shear zone. The modeled shear zone is bounded by undeformable wall rock and the deformation is applied in one event

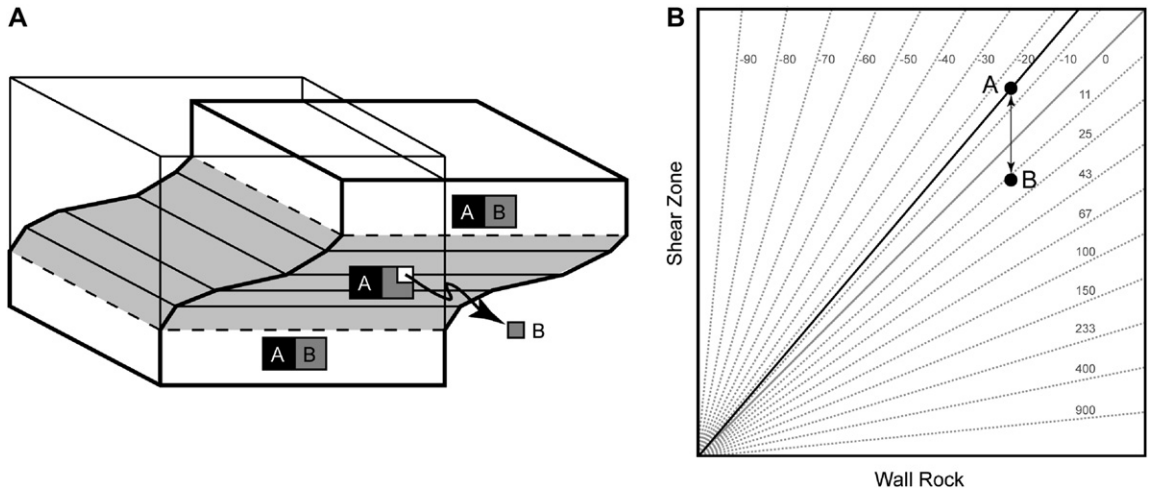

Fig. 4. (A) Schematic representation of volume loss from a two-component rock (modified from Hudleston, 1999). (B) Resulting isocon diagram when a quarter of B is lost during deformation, slope of the line fitted through the immobile A reveals $\Delta = -0.125$, or 12.5% of the volume is lost from the shear zone. Contours are the per cent volume change with respect to the identified immobile component.

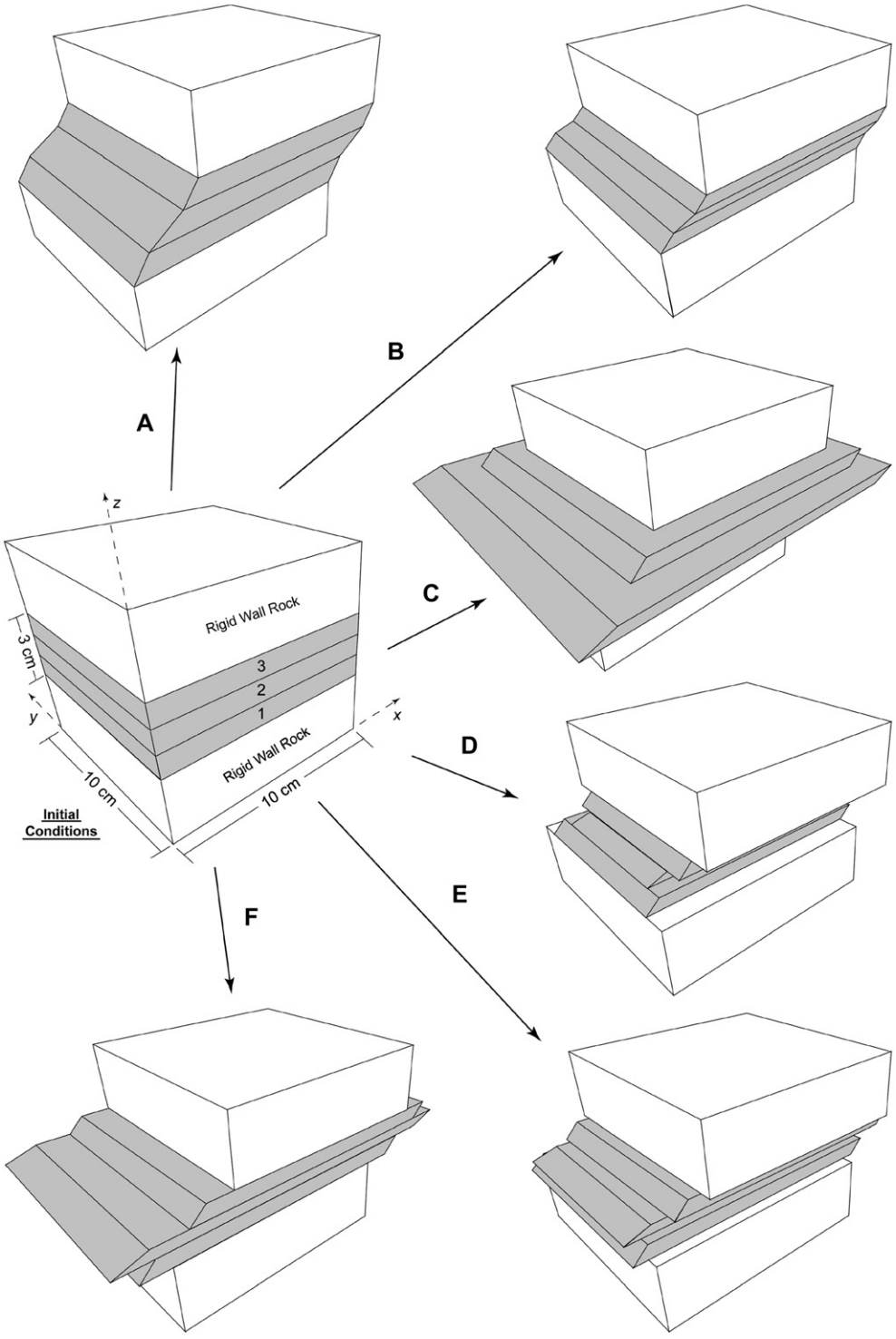

Fig. 5. Model initial condition with six scenarios of ductile shear zone formation. See text for details.

(Fig. 5). Deformation of multiple successive steps involving simple shear, pure shear, and volume loss, though possible in nature, is not considered. The bottom (Slice 1) and top slice (Slice 3) of the shear zone are deformed to half the total strain of Slice 2 (center of shear zone), but along the same strain path as Eq. (1). Therefore, the deformation matrix of Slice 1 and 3 relative to Slice 2 is (see Fossen and Tikoff, 1993):

$$D_{half} = \begin{bmatrix} k_x^{0.5} & 0 & 0.5\gamma \frac{\left(k_x^{0.5} - k_z^{0.5}\right)}{\ln\left(k_x^{0.5}/k_z^{0.5}\right)} \\ 0 & k_y^{0.5} & 0 \\ 0 & 0 & k_z^{0.5} \end{bmatrix} \tag{11}$$

Each of the three slices was deformed homogeneously by the requisite deformation matrix (Slice 2 by Eq. (1); Slice 1

Table 1
Parameters and characteristics of the shear zone models shown in Fig. 5

Scenario	k_x	k_y	k_z	Γ	γ	W_k	Shear zone thickness[a]	Shear zone displacement[a]	Shear zone vol. proportion[b]	$\sqrt{\lambda_1/\lambda_2}$[c]	$\sqrt{\lambda_2/\lambda_3}$[c]	R[c]	θ'[c]
A	1.000	1.000	1.000	1.500	1.500	1.000	3.0	3.0	1.00	2.00	2.00	4.00	26.6
B	1.000	1.000	0.300	0.872	1.500	0.661	1.4	2.0	0.47	1.34	4.47	6.00	8.7
C	1.493	1.493	0.448	1.302	1.500	0.763	1.8	2.7	1.00	1.34	4.47	6.00	8.7
D	1.000	0.650	0.300	0.872	1.500	0.661	1.4	2.0	0.36	2.06	2.91	6.00	8.7
E	1.240	0.806	0.372	1.082	1.500	0.724	1.6	2.3	0.53	2.06	2.91	6.00	8.7
F	1.539	1.000	0.462	1.342	1.500	0.768	1.8	2.7	0.80	2.07	2.91	6.00	8.7

[a] Though models are dimensionless, units are envisioned to be cm.
[b] Volume of entire shear zone following deformation (including extruded material).
[c] Flinn diagram and R-θ' states of strain for Slice 2.

and 3 by Eq. (11)) applied to the coordinates of the initial conditions (Fig. 5). Slices were stacked and pinned by their center points. Discontinuities therefore exist between each slice except at the center point of each slice. To more accurately represent natural shear zones, more slices could be used, but experimentation with such models that define a more realistic strain profile does not change the resulting characteristics of the models. The three-slice model used represents fairly well the high strained core of a shear zone surrounded by a moderately strained margin (Fig. 1B). Shear zone walls remain undeformed following the deformation.

Final thickness of a shear zone is the sum of the final thickness of each slice. Displacement (d) across any slice is simply the shear strain (γ) multiplied by the final thickness of the slice (t), therefore the total displacement across the shear zone walls relative to each other is:

$$d_{total} = \sum_{1}^{3} \gamma_i t_i. \tag{12}$$

3. Models

Six scenarios were modeled that are thought to describe many characteristics of shear zones reported in the literature. Table 1 contains all deformation matrix parameters and the resulting model characteristics. Fig. 5 displays accurate perspectives of the shear zone block models produced by using the deformation parameters of Table 1. The models assume that strain develops such that the incremental strain is constant across each slide of the shear zone and does not change during deformation. In all scenarios $\gamma = 1.5$, which is a value consistent with the strain analyses of Srivastava et al. (1995) and Bhattacharyya and Hudleston (2001). Other estimates of shear strain: $\gamma \approx 5$–20, by Ramsay and Graham (1970); $\gamma \approx 4$–7, by Ramsay and Allison (1979); $\gamma \approx 4$–7, by Simpson (1981); and $\gamma \approx 20$, by Mohanty and Ramsay (1994); probably overestimate γ if a pure shear component occurs (Simpson, 1981). Higher shear strains could have been modeled but the models become more cumbersome and shear zone characteristics essentially do not change. The particular choices of stretch (k_x, k_y, and k_z) and volume loss demonstrate a range of possible shear zone characteristics.

3.1. Scenario A

Scenario A (Fig. 5; Table 1) is the "classic" case of heterogeneous simple shear deformation, with no volume change. This style of deformation is commonly assumed, as strain compatibility is not a problem and volume is constant during deformation. However, shear zone terminations remains an issue for strain compatibility (as for all scenarios) and this issue has been addressed in some detail by, e.g. Ramsay and Allison (1979). The thickness of the shear zone is maintained throughout deformation and for a given shear strain (γ), displacement is the greatest compared to any other scenario that includes a flattening component (some combination of pure shear and volume loss). Because deformation is only by simple shear, $W_k = 1.0$. Strain on the R-θ', as described, falls on the $\Delta_{ap} = 0$ line (Fig. 6) and is plane strain on the Flinn diagram (Fig. 7). Providing the shear zone was not localized along a structure of different composition than the surrounding rock, there should be no bulk chemical differences between the wall rock and shear zone.

3.2. Scenario B

Another common assumption regarding the deformation within shear zones is that volume loss is the only mechanism that produces a narrowing or flattening across the shear zone during deformation. This is represented by Scenario B (Fig. 5; Table 1). Here, $\Delta_{ap} = -0.7$ (therefore $k_z = 0.300$; Fig. 6), which is fairly consistent with the strain analyses of Srivastava et al. (1995) and Bhattacharyya and Hudleston (2001). It is important to note that in this scenario $k_x = k_y = 1$, that is, with narrowing of the shear zone during deformation, the volume of the shear zone must be reduced. There is no net stretch in the x or y-direction, and therefore strain compatibility is not an issue. This deformation style reduces the thickness of the shear zone to 47% of that in Scenario A and reduces displacement to 67% of that in Scenario A (Table 1). Shear zones that deform by this style should display considerable bulk chemical differences between the wall rock and shear zone core. If a perfectly immobile reference frame can be identified, the isocon slope should be 3.3 (Eq. (10)). The state of finite strain on the Flinn diagram is the most

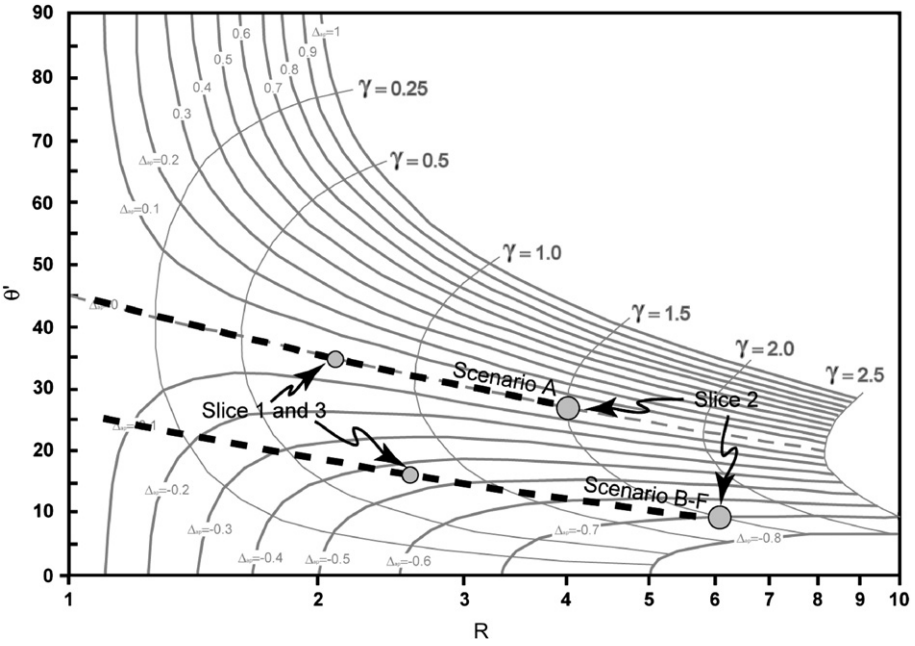

Fig. 6. R-θ' diagram for the various model scenarios. The complete strain path is shown as the thick dotted line, circles mark the finite strain of the various slices as labeled.

oblate of the strains considered in this analysis (Fig. 7). Flattening due to volume loss is a component of this deformation, so vorticity is less than 1, specifically, $W_k = 0.661$.

3.3. Scenario C

Scenario C (Fig. 5; Table 1) has identical strain to Scenario B (Figs. 6 and 7), but volume is maintained during deformation. The net result is that a significant amount of material must be extruded in all directions in the plane of the shear zone. Compared to Scenario B, vorticity ($W_k = 0.763$), shear zone thickness (1.8 cm), and displacement (2.7 cm) are all greater (Table 1). A version of Scenario C was scaled in the x and y-directions to be 1.0 m on a side to better approximate the real world geometry of shear zones (vertical scale is consistent with other models; Fig. 8). The extruded material from the shear zone extends 0.5 m beyond the limits of the wall rock in all directions after deformation. The actual volume of material extruded from a shear zone of this geometry is 1.2×10^4 cm^3. Scaling the model to 10 m in the initial x and y-directions produces a model with the extruded material extending 5 m beyond the limits of the undeformed wall rock and 1.2×10^6 cm^3 of extruded material. This emphasizes how the amount of extrusion is dependent on the lateral extent of a shear zone given that the other parameters remain fixed (i.e. strain and initial thickness). In general, this scenario approximates shear zones that have minimal bulk chemistry difference between the shear zone and wall rock, but have oblate strain.

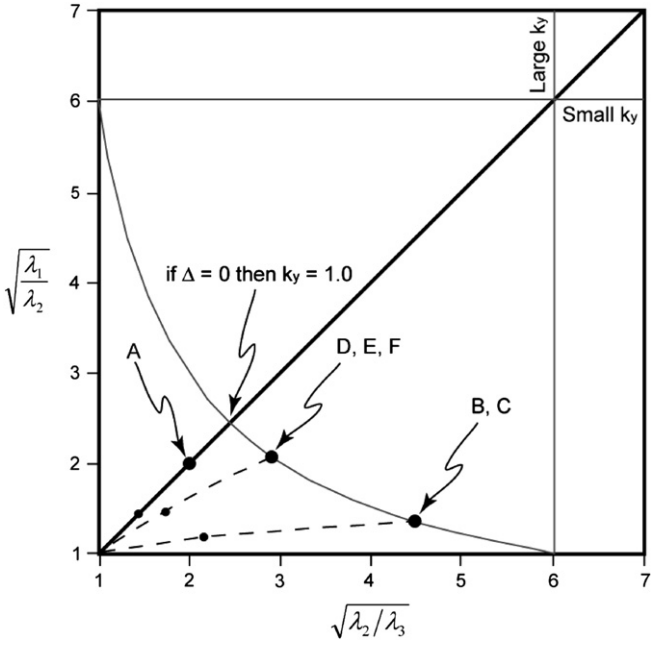

Fig. 7. Flinn diagram of all possible finite states of strain (gray line) for the model Scenarios B–F (Fig. 6). Strain for Scenario A has a different R-θ' to that of Scenarios B–F, therefore it does not lie on the gray line. Strain paths shown as dotted lines. Intermediate strains (finite strain of Slice 1 and 3) shown as points along the strain paths.

3.4. Scenario D–F

The last set of models explores the characteristics of models where $k_x \neq k_y$, specifically $k_x > k_y$ (Fig. 5; Table 1). Scenarios of $k_x < k_y$ can easily be envisioned but they are not addressed here and they produce Flinn diagram strains more oblate than Scenario B–C, if k_y is not extreme. With $k_x > k_y$, the shear zone x-dimension will always be greater than the y-dimension. The strains for Scenario D–F are identical to one another (Figs. 6 and 7), but are less oblate than the strains of Scenario B–C. Scenarios D–F differ from one

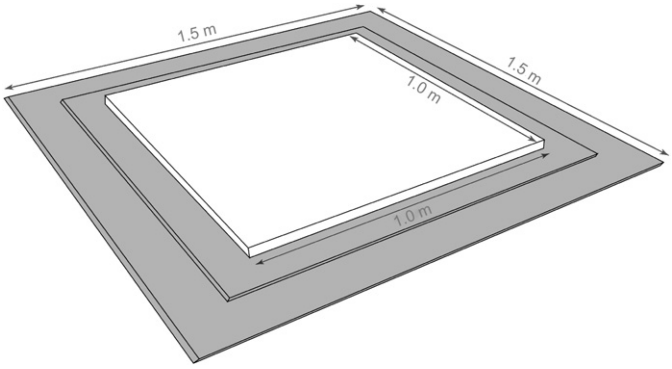

Fig. 8. Model Scenario C scaled to the initial x- and y-dimensions of 1 meter, initial thickness (z-dimension) is the same as the Scenario C model of Fig. 5.

another only in the amount of volume change. Scenario D fixes $k_x = 1$, such that no material is extruded in the direction of shear, which necessitates the intrusion of material into the sides of the shear zone for bulk strain compatibility. Scenario E is constrained to no net extrusion, that is, the amount of material extruded in the direction of shear is equalized by the amount of material that needs to be intruded into the sides of the shear zone to maintain overall strain compatibility. Scenario F fixes $k_y = 1$ so material must be extruded in the direction of shear to produce the same relative strain as Scenario D and E. In Scenario D–F, volume loss occurs (−64%, −47%, and −20% respectively) and the isocon plots for shear zones of these types should display chemical variations representative of such volume losses. Shear zones of this type always require extrusion/intrusion regardless of the volume loss of the shear zone, as is the case of $k_x < k_y$ shear zones.

4. Discussion

The results of the modeling described above reveal a number of important aspects regarding the specifics of ductile shear zone deformation that includes flattening. Specifically, for a given relative strain, volume change is independent of the ellipsoid shape and volume change needs to be constrained to fully characterize all aspects of shear zone deformation. Volume change strongly influences the vorticity, final shear zone thickness, displacement, and geometry (Fig. 5; Table 1), demonstrated by Fig. 9. The graphed thickness and displacements of Fig. 9 are specific to the 3 slice model used here and are normalized to the results of Scenario A with $\Delta = 0$. The three parameters are somewhat insensitive to the amount of volume change except at large volume losses. In general, the less volume loss there is, given the same initial conditions, the thicker the zone is and the greater the displacement. Fig. 9A shows that for the specifics of that model (simple shear deformation only), vorticity is maximum at no volume change and decreases with either increasing or decreasing volumes during deformation. Fig. 9B demonstrates that if Δ_{ap} is <1, regardless of Δ, W_k will be less than 1.

These results also demonstrate that only one type of deformation produces flattening strains that do not require extrusion.

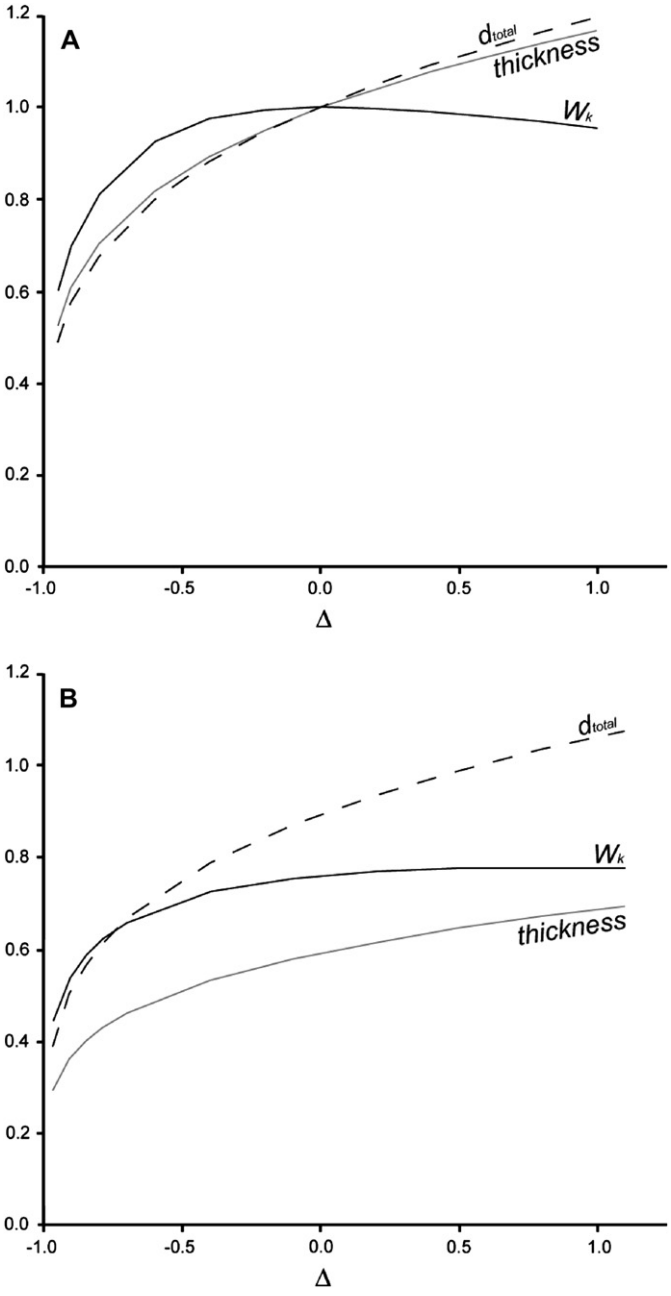

Fig. 9. Relationship between volume change (Δ) and vorticity (W_k), normalized shear zone thickness, and normalized displacement (d_{total}). $\Delta < 0$ denotes volume loss, $\Delta > 0$ denotes volume gain. (A) Parameter variation for the strain of Scenario A (Fig. 5; Table 1). (B) Parameter variation for the strain of Scenario B and C (Fig. 5; Table 1).

Scenarios A and B both have the common characteristic of $k_x = k_y = 1$, which is required for there not to be extrusion, therefore in this situation, $k_z = (1 + \Delta_{ap}) = (1 + \Delta)$. Here, volume loss is the only mechanism producing the flattening component of the deformation.

If the constraint of no extrusion is imposed/assumed, then a Flinn diagram can be contoured for values of γ and k_z, where $k_z = (1 + \Delta_{ap}) = (1 + \Delta)$, and $k_x = k_y = 1$ (Fig. 10). So for any given state of strain on a R-θ' diagram below the $\Delta_{ap} = 0$ line, there is only one corresponding Flinn diagram oblate state of

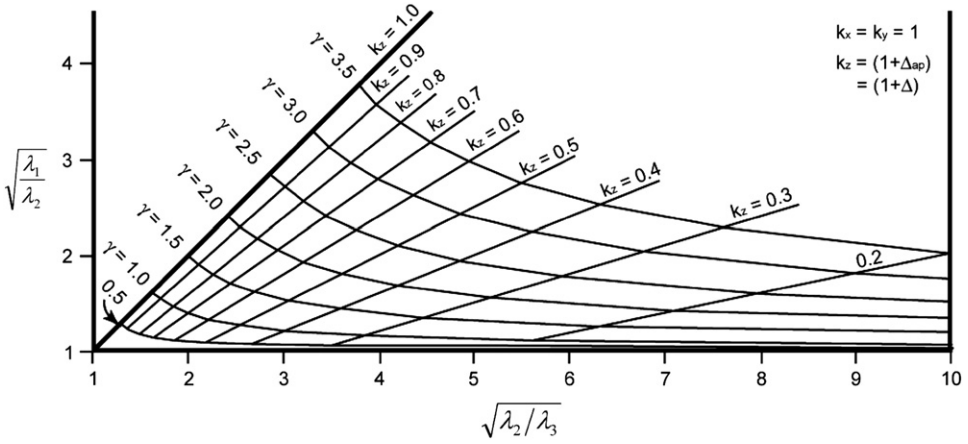

Fig. 10. Flinn diagram contoured for flattening strains where only volume loss is responsible for the z-axis parallel flattening.

strain and corresponding volume loss that will yield a shear zone without extrusion (Fig. 10). Therefore, even without accurate volume loss estimates from the isocon method, the degree of extrusion can be assessed by the Flinn diagram state of strain relative to the R-θ' state of strain (c.f. Schwerdtner, 1982). That is, if $k_x \neq k_y$, γ will not agree between the R-θ' diagram (Fig. 2) and the contoured Flinn diagram (Fig. 10). Mohanty and Ramsay (1994) provide an equation that solves for Δ from the Flinn diagram's state of strain, assuming $k_x = k_y = 1$:

$$\Delta = \frac{\sqrt{\lambda_1}/\sqrt{\lambda_2}}{\sqrt{\lambda_2}/\sqrt{\lambda_3}} - 1. \tag{13}$$

This equation alone cannot constrain γ or assess the existence of extrusion without comparing the calculated Δ (Eq. (13)) to Δ_{ap}.

Extrusion is required if there are significant discrepancies between the isocon volume loss estimate and the geometric volume loss (Fig. 10; Eq. (13)) as demonstrated by the difference in Scenario B and C (Fig. 5). This is the case for the strain data of Bhattacharyya and Hudleston (2001), whose data requires extrusion/intrusion irrespective of the volume loss ($k_x < k_y$, see above). Therefore, to truly assess the relative roles of extrusion and volume loss in a shear zone, a full 3D strain analysis must be obtained with an independent estimate of volume change – typically the isocon method as described above. Absolute strain analysis can provide this information but these are often very hard to conduct.

4.1. Strain analysis

Much of the present argument rests on the ability to obtain accurate, complete, strain data accompanied by accurate volume change estimations. Problems with volume change estimations have been described above. A quality strain analysis requires two major assumptions to be fulfilled: (1) features within a rock can be used to measure strain, typically these are approximately ellipsoidal markers, although markers of other shape may suffice (e.g. Robin, 1977). (2) The strain markers must accurately record the strain and behave passively, with no competency contrast existing within the rocks. Shear zones can be commonly found in igneous rocks, which can provide enclaves (e.g. Simpson, 1981; Choukroune and Gapais, 1983) and relict igneous grains (Srivastava et al., 1995; Bhattacharyya and Hudleston, 2001) for strain analysis.

Though inaccuracies in strain analyses exist, it is difficult to determine to what extent previously reported strain analyses might be systematically incorrect. That is, prior strain analyses could be biased as to indicate a spurious pure shear component to the deformation, as opposed to simple shear only, providing the system is isochoric. In general, an obvious systematic error could be the underestimation of the aspect ratio of the xz-plane ellipse given that the θ' measurements are unbiased. If strain is produced by simple shear only, this error will produce a measured strain off the $\Delta_{ap} = 0$ line into regions suggesting a flattening component. Ramifications of this type of error are not as obvious on the Flinn diagram and cannot be predicted without the specifics of the strain analysis known. If the strain in the xz-plane is incorrect, it is reasonable to assume that the strain measured in any other plane is incorrect as well. The erroneous strain can then be of any shape depending upon the relative error in the measured planes. In general it seems unlikely that an easily identifiable systematic error could explain all strain data. A wide range of techniques on various lithologies have been used suggesting legitimacy to the flattening component of deformation commonly reported in the literature. Therefore, we conclude that a flattening component to shear zone formation is a common occurrence.

4.2. Extrusion

Stretching lineation orientations perpendicular to the transport direction in crustal-scale shear zones indicate transpression and the extrusion of material (e.g. Hudleston et al., 1988; Tikoff and Greene, 1997). In some cases, lineations can be oblique to the transport direction indicating triclinic deformation (e.g. Jiang and Williams, 1998; Czeck and Hudleston, 2003, 2004). Similar evidence for extrusion can be found in shear zones that even possess volume loss. Good examples of this are Simpson (1981; utilizing the conclusions of

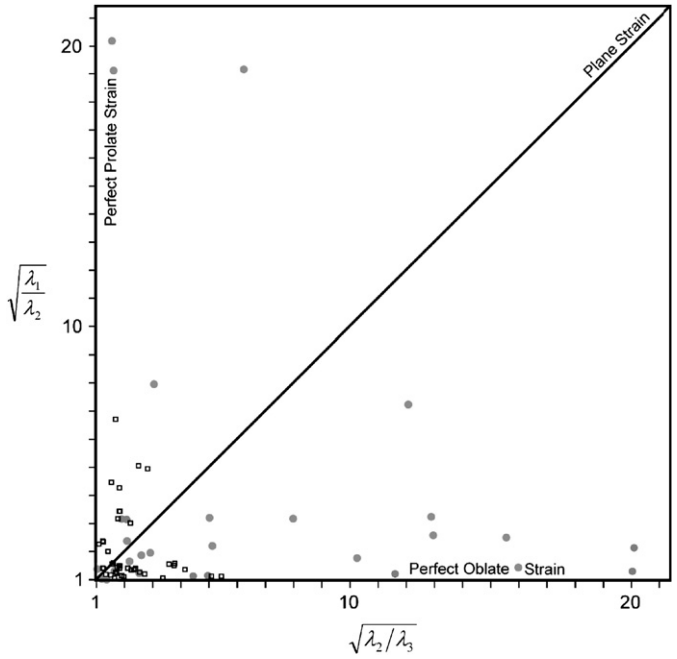

Fig. 11. Flinn diagram of the strain within the Maggia Nappe, the Alps (circles, from Simpson, 1981) and three samples from the Seve Nappe in northern Sweden (squares; from Bhattacharyya, 2000).

Mohanty and Ramsay, 1994) and Ring (1999), who both describe lineation attitudes perpendicular to the shear directions. Bhattacharyya and Hudleston (2001) report strain from shear zones that probably do not exhibit volume loss (c.f. Srivastiva et al., 1995; Baird, 2006), and demonstrate that the average length of the feldspar aggregates used as strain markers in their study increase in the *yz*-plane and decrease in the *xz*-plane. They interpret this as indicating extrusion.

Crustal-scale transpressive zones possess a free surface, so extrusion, and therefore true/apparent volume loss, is less of a concern to maintain bulk strain compatibility. Meso-scale ductile shear zones do not have the luxury of a free surface so extruded material has to be accommodated in some way to maintain strain compatibility. Hudleston (1999) suggested that extrusion in shear zones can be accommodated by the linking together of shear zones into arrays in which oblate strained shear zones extruding material are paired with prolate strained shear zones (requires the intrusion of material) to maintain strain compatibility. The linking of shear zones is common (e.g. Chourkoune and Gapais, 1983; Mitra, 1979; Simpson, 1981; Carreras, 2001), and some natural systems do contain both prolate and oblate strained shear zones (Fig. 11; see Simpson, 1981; Bhattacharyya, 2000) lending credence to this notion. Caution, however, should be taken when interpreting this strain data.

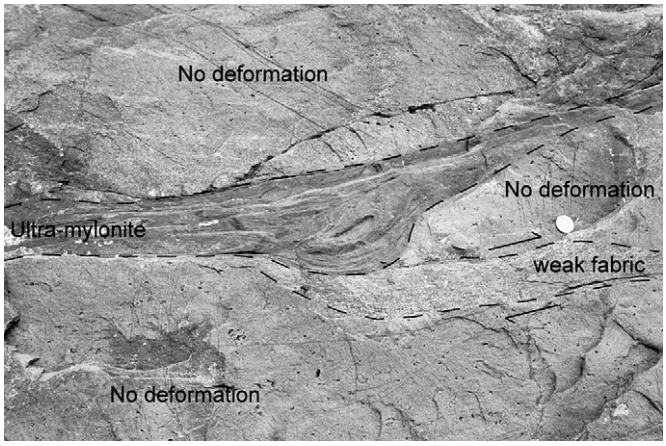

Fig. 13. Field evidence of extrusion in non-parallel-sided shear zones from Tarfala, Sweden. Outcrop has minimal topography and is approximately perpendicular to the shear zone and parallel to regional shear direction. Five Kronor piece is 29 mm across.

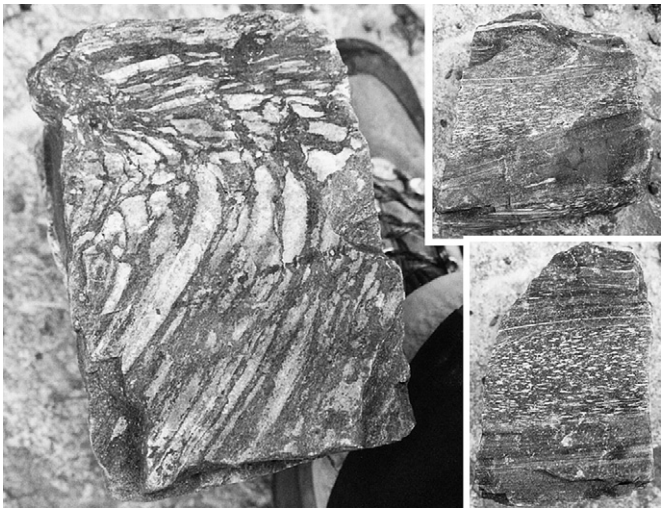

Fig. 12. Loose boulder fractured parallel to foliation that displays stretched plagioclase aggregates defining a stretching lineation with variable trajectory and character (Tarfala Valley, Sweden). Sample width approximate 13 cm. Insets show two foliation perpendicular views of the boulder.

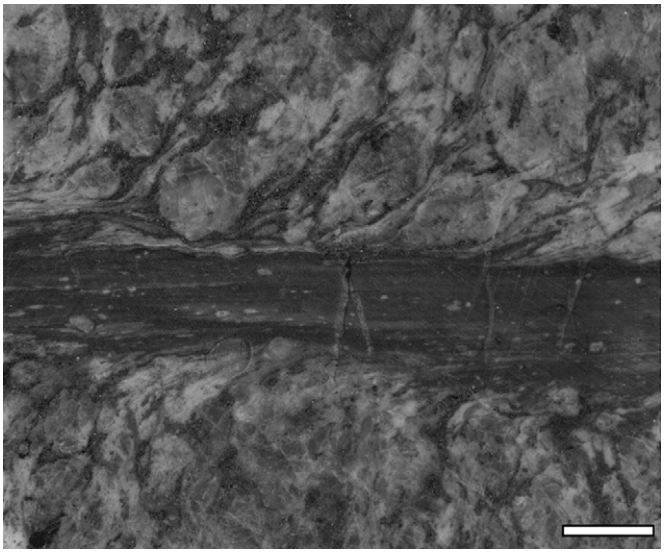

Fig. 14. Slabbed shear zone from the Diana Syenite of the northwest Adirondacks, scale bar is 1 cm. Shear zones in this area are typically straight, parallel-sided, and laterally extensive.

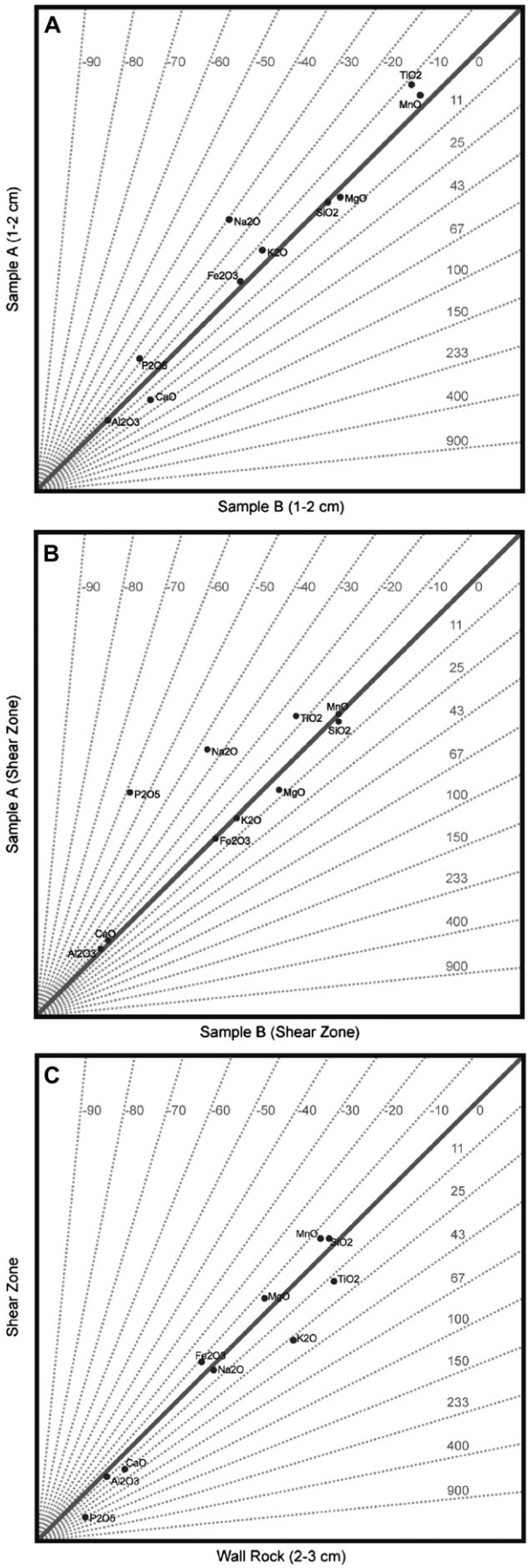

Fig. 15. (A) Isocon diagram for sample shown in Fig. 14. (B, C) Comparison of bulk chemistry from redundant portions of the same sample. Distance measurements indicate location of sample relative to the shear zone.

The Hudleston (1999) model, and the model presented here, assumes shear zones are straight and have parallel sides, however, natural shear zones could have non-parallel sides. Undulations in the sides necessitate the lateral movement of material within an individual shear zone without the need for the interconnection of shear zones. Volume loss could play a role in this as has been demonstrated at the regional scale by Newman and Mitra (1993), but at the scale of interest in this work, volume loss probably would be constant throughout the shear zone system. In a simplistic view, if no volume loss occurs, where shear zones thicken constrictional strain should be observed; while thinner portions of shear zones should have flattening strains (see Passchier, 1998). However triclinic shear zones may be common in some systems resulting in much more complex strain patterns than this simple view can give justice to. If volume loss occurs, then strain may not be as straightforward, depending upon the contribution of volume loss and stretch to the strain. Development of thickness changes could be produced by structures analogous to restraining and releasing bends in strike-slip.

Mandal et al. (2001) theoretically modeled the extrusion of material from transpressive shear zones and demonstrated that for laterally extensive shear zones, the deformation has to be close to simple shear. This is consistent with the findings of this work where it is shown that a modeled laterally extensive shear zone (Fig. 8) produces what is an unreasonable amount of extruded material, if volume is constant. However, for shear zones with low length to width ratios, extrusion is permissible (Mandal et al., 2001; Scenario C of Fig. 5 vs. Fig. 8). This suggests that in shear zone systems where extrusion occurs, shear zones are likely to be of fairly short length and be interconnected. Shear zones do not have to interlink, but shear zone thickness must then vary at fairly short scales.

Prolate strains should be fairly prevalent and associated with shear zones if indeed material is extruded from oblate strained portions of shear zones – so commonly reported in the literature. However, few reports of prolate strain exist. This discrepancy could be due to a sampling bias, where the oblate strained areas are much more laterally extensive, while the prolate strained zones are less so and may possess fabrics less conducive to proper strain analysis due to complex fabric patterns (see below).

Field evidence from shear zones in the Tarfala region of the northern Swedish Caledonides (Srivastava et al., 1995; Bhattacharyya and Hudleston, 2001; Baird, 2006) demonstrates unequivocally that the lateral movement of material occurred within these ductile shear zones (Figs. 12 and 13). Fig. 12 shows a section parallel to the foliation from this location that has been fractured parallel to foliation. A stretching lineation is defined by elongate plagioclase aggregates and has a curving character. It appears to be a natural example of the results of the physical experiment by Czeck and Hudleston (2004), where lineations oblique to the transport direction were produced by a ''leak'' in their squeeze box apparatus. Fig. 13 displays an example of ''swirled'' ultra-mylonite fabric within thicker portions of shear zones at Tarfala. This fabric is probably caused by the lateral movement of material into these thickened zones. In this example, the thicker portion is created by the intersection of shear zones. Complex fabrics in high shear regions such as this have also been described by Fossen and Rykkelid (1990).

In contrast to the Swedish shear zones, the shear zones in the Diana Syenite of the northwest Adirondacks (New York) are very different in character (Baird, 2006). Apart from local complications, in general, the shear zones are solitary, straight, and parallel-sided (Fig. 14). Bulk chemistry from one Adirondack sample, determined by the standard technique of $LiBO_2$ fusion of rock powders, HCl dissolution, and ICP-MS analysis, shows no evidence for volume loss as, in particular, SiO_2 and Al_2O_3 are in equal concentrations between the wall rock and shear zone (Fig. 15). Any scatter in the data (Fig. 15A) is similar to the scatter observed between separate analyses taken from the same relative location with respect to the shear zone (Figs. 15B, C; Baird, 2005). Therefore, deformation must be only by simple shear apart from the noted local complications. In rare instances, these shear zones interlink, but this does not require extrusion/intrusion, the interlinking is only a strain accommodation mechanism.

5. Conclusions

The models presented here show that volume loss is an important phenomenon in shear zones, and one that has significant control of shear zone thickness, displacement, and vorticity. Volume loss, however, cannot be constrained from most strain analyses. We demonstrate that, even if evidence for volume loss occurs (as estimated by the isocon method or by absolute strain measurements), this does not exclude extrusion from accompanying the development of a shear zone. For a given volume loss, there is only one specific strain orientation and geometry that satisfies the condition of no extrusion. In nature, evidence for extrusion, independent of strain data, can be found. This work and the work of others suggest that lateral displacement of material must be over fairly short distances, and straight, parallel-sided, laterally extensive shear zones must be developed by simple shear if volume loss is insignificant. Extruded material can either move within interlinked anastomosing shear zone arrays of prolate and oblate strains, or from thinned portions (oblate strain) of solitary shear zones to thicker portions (prolate strain).

Acknowledgements

The Tarfala Research Station of Stockholm University is thanked for very comfortable accommodations during field investigations of the shear zones in the area. UMN Department of Geology and Geophysics Summer Research Grants partially supported the fieldwork in Tarfala. GBB thanks Keith A. Brugger for valuable field assistance in Sweden. Fieldwork in the Adirondacks was partially supported by a Geological Society of America Graduate Student Research Grant (7327-03) to GBB. Much of the modeling work was accomplished while GBB was funded by the Graduate Assistance in Areas of

National Need Fellowship provided by the U.S. Department of Education. Annia Fayon is thanked for her review of an early draft of this paper. Haakon Fossen and Scott Giorgis are thanked for their careful and insightful reviews that greatly improved the manuscript.

References

Baird, G.B., 2005. Chemistry variations and volume loss in meso-scale ductile shear zones: example from the northwest Adirondacks, New York. Abstracts with Programs – Geological Society of America 37 (5), 5.

Baird, G.B., 2006. The strain and geometry of meso-scale ductile shear zones and the associated fluid flow. Ph.D. thesis, University of Minnesota.

Bhattacharyya, P., 2000. Shear zones of northern Swedish Caledonides. Ph.D. thesis, University of Minnesota.

Bhattacharyya, P., Hudleston, P., 2001. Strain in ductile shear zones in the Caledonides of northern Sweden: a three-dimensional puzzle. Journal of Structural Geology 23, 1549–1565.

Carreras, J., 2001. Zooming on Northern Cap de Creus shear zones. Journal of Structural Geology 23, 1457–1486.

Choukroune, P., Gapais, D., 1983. Strain pattern in the Aar Granite (Central Alps): orthogneiss developed by bulk inhomogeneous flattening. Journal of Structural Geology 5, 411–418.

Cobbold, P.R., 1977. Description and origin of banded deformation structures. I. Regional strain, local perturbations, and deformation bands. Canadian Journal of Earth Sciences 14, 1721–1731.

Coward, M.P., 1976. Strain within ductile shear zones. Tectonophysics 34, 181–197.

Czeck, D.M., Hudleston, P.J., 2003. Testing models for obliquely plunging lineations in transpression: a natural example and theoretical discussion. Journal of Structural Geology 25, 959–982.

Czeck, D.M., Hudleston, P.J., 2004. Physical experiments of vertical transpression with localized nonvertical extrusion. Journal of Structural Geology 26, 573–581.

Dutton, B.J., 1997. Finite strains in transpression zones with no boundary slip. Journal of Structural Geology 19, 1189–1200.

Etheridge, M.A., Wall, V.J., Vernon, R.H., 1983. The role of the fluid phase during regional metamorphism and deformation. Journal of Metamorphic Geology 1, 205–226.

Fossen, H., Rykkelid, E., 1990. Shear zone structures in the Øygarden area, West Norway. Tectonophysics 174, 385–397.

Fossen, H., Tikoff, B., 1993. The deformation matrix for simultaneous simple shearing, pure shearing and volume change, and its application to transpression-transtension tectonics. Journal of Structural Geology 15, 413–422.

Fossen, H., Tikoff, B., Teyssier, C., 1994. Strain modeling of transpressional and transtensional deformation. Norsk Geologisk Tidsskrift 74, 134–145.

Grant, J.A., 1986. The isocon diagram – a simple solution to Gresens' equation for metasomatic alteration. Economic Geology 81, 1976–1982.

Grunsky, E.C., Robin, P.-Y.F., Schwerdtner, W.M., 1980. Orientation of feldspar porphyroclasts in mylonite samples from the southern Churchill Province, Canadian Shield. Tectonophysics 66, 213–224.

Hudleston, P., 1999. Strain compatibility and shear zones: is there a problem? Journal of Structural Geology 21, 923–932.

Hudleston, P.J., Schultz-Ela, D., Southwick, D.L., 1988. Transpression in an Archean greenstone belt, northern Minnesota. Canadian Journal of Earth Science 25, 1060–1068.

Jiang, D., Williams, P.F., 1998. High-strain zones: a unified model. Journal of Structural Geology 20, 1105–1120.

Jones, R.R., Holdsworth, R.E., Bailey, W., 1997. Lateral extrusion in transpression zones: the importance of boundary conditions. Journal of Structural Geology 19, 1201–1217.

Lisle, R.L., 1985. Geological Strain Analysis: a Manual for the Rf/Φ Technique. Pergamon Press, Oxford.

Mandal, N., Chakraborty, C., Sammanta, S.K., 2001. Flattening in shear zones under constant volume: a theoretical evaluation. Journal of Structural Geology 23, 1771–1780.

Mitra, G., 1979. Ductile deformation zones in Blue Ridge basement rocks and estimation of finite strains. Geological Society of America Bulletin 90, 935–951.

Mohanty, S., Ramsay, J.G., 1994. Strain partitioning in ductile shear zones: an example from a Lower Pennine nappe of Switzerland. Journal of Structural Geology 16, 663–676.

Newman, J., Mitra, G., 1993. Lateral variations in mylonite zone thickness as influenced by fluid-rock interactions, Linville Falls fault, North Carolina. Journal of Structural Geology 15, 849–863.

O'Hara, K., 1990. State of strain in mylonites from the western Blue Ridge province, southern Appalachians: the role of volume loss. Journal of Structural Geology 12, 419–430.

Passchier, C.W., 1998. Monoclinic model shear zones. Journal of Structural Geology 20, 1121–1137.

Ramberg, H., 1975. Particle paths, displacement and progressive strain application to rocks. Tectonophysics 28, 1–37.

Ramsay, J.G., 1980. Shear zone geometry: a review. Journal of Structural Geology 2, 83–99.

Ramsay, J.G., Allison, I., 1979. Structural analysis of shear zones in an alpinised Hercynian granite (Maggia Lappen, Pennine Zone, Central Alps). Schweizerische Mineralogische und Petrographische Mitteilungen 59, 251–279.

Ramsay, J.G., Graham, R.H., 1970. Strain variation in shear belts. Canadian Journal of Earth Sciences 7, 786–813.

Ramsay, J.G., Huber, M.I., 1987. The Techniques of Modern Structural Geology. In: Folds and Fractures, Vol. 2. Academic Press, London.

Ring, U., 1999. Volume loss, fluid flow, and coaxial versus noncoaxial deformation in retrograde, amphibolite facies shear zones, northern Malawi, east-central Africa. Geological Society of America Bulletin 111, 123–142.

Robin, P.-Y.F., 1977. Determination of geologic strain using randomly oriented strain markers of any shape. Tectonophysics 42, T7–T16.

Robin, P.-Y.F., Cruden, A.R., 1994. Strain and vorticity patterns in ideally ductile transpression zones. Journal of Structural Geology 16, 447–466.

Sanderson, D.J., Marchini, W.R.D., 1984. Transpression. Journal of Structural Geology 6, 449–458.

Schwerdtner, W.M., 1982. Calculation of volume change in ductile band structures. Journal of Structural Geology 4, 57–62.

Simpson, C., 1981. Ductile shear zones: a mechanism of rock deformation in the orthogneisses of the Maggia Nappe, Ticino. Ph.D. thesis, ETH Zurich.

Simpson, C., 1983. Strain and shape-fabric variations associated with ductile shear zones. Journal of Structural Geology 5, 61–72.

Srivastava, H.B., Hudleston, P., Earley III, D., 1995. Strain and possible volume loss in a high-grade ductile shear zone. Journal of Structural Geology 17, 1217–1231.

Teyssier, C., Tikoff, B., 1999. Fabric stability in oblique convergence and divergence. Journal of Structural Geology 21, 969–974.

Tikoff, B., Fossen, H., 1993. Simultaneous pure and simple shear: the unifying deformation matrix. Tectonophysics 217, 267–283.

Tikoff, B., Fossen, H., 1999. Three-dimensional reference deformations and strain facies. Journal of Structural Geology 21, 1497–1512.

Tikoff, B., Greene, D., 1997. Stretching lineations in transpressional shear zones: an example from the Sierra Nevada Batholith, California. Journal of Structural Geology 19, 29–39.

Yonkee, W.A., Parry, W.T., Bruhn, R.L., 2003. Relations between progressive deformation and fluid-rock interaction during shear-zone growth in a basement-cored thrust sheet, Sevier Orogenic Belt, Utah. American Journal of Science 303, 1–59.